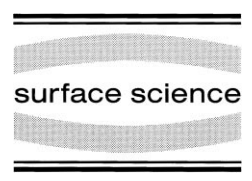


Surface Science 432 (1999) 305–315



www.elsevier.nl/locate/susc

# A density functional theory study on the interaction between chemisorbed CO and S on Rh(111)

C.J. Zhang a, P. Hu a,\*, M.-H. Lee b

<sup>a</sup> School of Chemistry, The Queen's University of Belfast, Belfast BT9 5AG, UK <sup>b</sup> Department of Physics, Tamkang University, Tamsui 25137, Taiwan

Received 5 February 1999; accepted for publication 22 April 1999

## Abstract

Density functional theory calculations are carried out for Rh(111)-p( $2 \times 2$ )-CO, Rh(111)-p( $2 \times 2$ )-S, Rh(111)-p( $2 \times 2$ )-CO, Rh(111)-p( $3 \times 3$ )-CO, Rh(111)-p( $3 \times 3$ )-S and Rh(111)-p( $3 \times 3$ )-(S+CO), aiming to shed some light on the S poisoning effect. Geometrical structures of these systems are optimized and chemisorption energies are determined. The presence of S does not significantly influence the geometrical structure and chemisorption energy of CO and vice versa, which strongly suggests that the interaction between CO and S on the Rh(111) surface is mainly short-range in nature. The long range electronic effect for the dramatic attenuation of the CO methanation activity by sulfur is likely to be incorrect. It is suggested that an ensemble effect may be dominant in the catalytic deactivation. © 1999 Elsevier Science B.V. All rights reserved.

Keywords: Carbon monoxide; Density functional calculations; Poisoning effects; Rhodium; Sulfur

# 1. Introduction

Sulfur is well known to be poisonous for the CO methanation reaction [1]. The addition of 0.1 monolayer (ML) of sulphur can cause drastic reduction in the rate of CO methanation over Ni(100), Rh(111) and Ru(001). The interaction between S and CO coexisting on metal surfaces has been the focus of many experimental and theoretical investigations. However, the mechanisms responsible for such poisoning effects are still not well understood [2]. In this study, we report some results of density functional theory calculations in order to shed light on this issue.

Goodman and Kiskinova [3–5] carried out sub-

tronegative atoms such as Cl, S and P on the adsorption of CO on Ni(100) using thermal desorption (TD), low energy electron spectroscopy (LEED) and Auger electron spectroscopy (AES). They suggested that the reductions in CO saturation coverage by preadsorbed Cl, S and P atoms could be accounted for by differences in the electronegativity of the adatom: the higher the electronegativity, the more pronounced the poisoning effect is. Kinetic studies [4] were also performed for CO methanation on Ni(100) covered with sulfur and phosphorus. According to the initial attenuation of the catalytic activity by these impurities, they estimated that each S atom on Ni(100) poisons ten or more sites for the reaction of CO with H<sub>2</sub> to form CH<sub>4</sub> and only the four nearest neighbour

nickel atom sites are deactivated by one P atom.

stantial studies on the effects of preadsorbed elec-

<sup>\*</sup> Corresponding author. Fax: +44-1232-382117. E-mail address: p.hu@qub.ac.uk (P. Hu)

Therefore, they concluded that an extended electron effect is dominant in catalytic deactivation by sulfur. Experimental studies of S and CO coadsorbed on Ni(111) [6], Rh(111) [7] and Ru(001) [8] also supported this type of long-range interaction.

However, from an experimental work also with S and CO on Ni(100), Madix et al. [9] drew the opposite conclusion that the sulfur influences CO chemisorption on Ni(100) through a local interaction. They observed that:

- very little difference appears between the ability of Cl and S to reduce CO saturation coverage;
- the binding energy of CO which desorbs from the high temperature state is not altered by S more than it will be by a similar increase in CO coverage.

These results were hardly consistent with long range interaction. From a vibrational characterization of CO adsorbed on sulfur-modified Ni(100) surfaces, Gland et al. [10] also suggested the S-CO interaction is predominantly local. The same conclusion was obtained by Trenary et al. [11]. Recently, a study on the interaction between coadsorbed CO with sulfur on Ni(110) using room temperature scanning tunnelling microscopy (STM) and LEED [12] showed that a short-range repulsive interaction is largely responsible for the observed segregation of the constituent adatoms into small domain islands.

Theoretically, studies have been performed in order to understand the poisoning of sulfur. Feibelman and Hamann [13,14] have carried out self-consistent linearized-augmented-plane-wave calculations on the electronic structure perturbations induced by sulfur on the Rh(100) surface. They found that S-induced charge density vanishes beyond the adjacent Rh atoms but that the local density of states (LDOS) near the Fermi level is substantially reduced by S even beyond the next nearest neighbour Rh atoms. The extent of the poisoning effect of sulfur has also been studied by Maclaren and Pendry [15] by using Green's function formalism and the muffin-tin approximation applied to clusters for an S-modified Rh(111) surface. The effective range was estimated to be < 5 Å. A theoretical model was proposed by Lang and colleagues [16,17] who explained the effect of the additives by the sign and magnitude of the electrostatic potential around the adatom on a jellium surface. Based on self-consistent calculations of the electronic structures of adsorbed electronegative atoms, they showed that the increase of the poisoning strength in the sequence P, S, Cl is related to their different electrostatic potentials in the same direction. The range of these interactions was estimated to be <4 Å. Wimmer et al. [18] studied, for the first time, the coadsorption system, Ni(100)-c(2 $\times$ 2)-(S+CO), using an allelectron full-potential linearized-augmented-planewave method, and concluded that the poisoning effect of S has a complex nature involving covalent bonding between S and the Ni surface accompanied by a small transfer of electronic charge towards the S atoms as well as direct interactions between S and adjacent CO molecules. The dissociation of hydrogen molecules on metal surfaces is an important step in the CO methanation reaction. The poisoning effect of S on hydrogen dissociation has been studied by Wilke and Scheffler [19,20]. Through an investigation on the potential energy surface of  $H_2$  dissociation on Pd(100)-p(2×2)-S, they presented that the poisoning effect of S originates from the formation of an energy barrier hampering the H<sub>2</sub> dissociation.

It is clear that further studies on the interaction of adsorbates are required. In particular, the poisoning effect of S on CO methanation needs to be further examined in light of the debate on the issue [2]. In this study, we chose CO coadsorption with S on the Rh(111) surface. We first carried out ab initio total energy calculations using density functional theory on Rh(111)-p(2 $\times$ 2)-CO, Rh(111) $p(2 \times 2)$ -S and Rh(111)- $p(2 \times 2)$ -(S+CO). We compared the adsorption geometries of single species with those in the coadsorption system, which should provide some insight into the sulfur poisoning effect. We noted that a very low coverage (about 0.1 monolayer) of S can cause drastic reduction of the rate of CO methanation. Therefore, in order to further determine the S-CO interaction and explain the reduction of methanation rate, a large unit cell is required to investigate. It is with this motivation that we also performed ab initio total energy calculations with DFT for Rh(111)-  $p(3 \times 3)$ -CO, Rh(111)- $p(3 \times 3)$ -S and Rh(111)- $p(3 \times 3)$ -(S+CO). To identify the origin of the poisoning effect of S in more detail, we also analyzed the electronic structures. Since the lateral interaction between adsorbates is one of the key mechanisms affecting chemical reactions on surfaces and in catalysis, we hope the present study may shed some light on the catalytic deactivation mechanism.

## 2. Calculations

We carried out ab initio total energy calculations using density functional theory. A density mixing scheme was employed to determine the electronic ground states. The electronic wave functions were expanded in a plane wave basis set. Ionic cores were described with ultrasoft pseudopotentials, which were generated using the scheme proposed by Vanderbilt [21]. This allows the use of a very small number of plane waves to describe the valence wave functions. A cut-off energy of 300 eV was found to be sufficient and two k-points in the two-dimensional Brillouin zone were used. The metal substrate was modelled by a slab of three layers, each slab separated by a 10 Å vacuum region. In the calculations, the metal substrate was fixed whereas C, O and S atoms were allowed to move in all directions to lower the energies according to the forces calculated using the Hellmann-Feynman theorem.

Recent studies [22–24] have shown that geometrical structures of molecules and solids determined by local density approximation (LDA) [25] calculations are very reasonable compared to experiwork and that no considerable improvement is obtained using gradient corrections. On the other hand, chemisorption energies obtained using LDA are significantly higher than experimental values, while calculation results with gradient corrections agree with experimental data very well. Thus, we used LDA to obtain adsorption geometries, and for the calculation of chemisorption energies, we employed the generalized gradient approximation (GGA) [26]. In the LDA, the Ceperly-Alder exchange-correction energy was

used while the GGA of Perdew–Wang was utilized in the gradient correction calculations.

The calculation results accurately reproduced the properties of the isolated systems, including the equilibrium lattice constant of Rh and the CO bond length. Using DFT–LDA, the Rh bulk lattice constant was determined to be 3.804 Å (error 0.1%), and the bond length of CO was found to be 1.146 Å (error 1.6%).

# 3. Results

Recently the geometrical structure of S on Rh(111) single crystal surface has been investigated using several techniques including LEED, STM, normal incidence X-ray standing wavefield (NIXSW) and surface-extended X-ray absorption fine structure (SEXAFS) [27-29]. Five ordered overlayer structures were observed in the LEED experiment [27]:  $(\sqrt{3} \times \sqrt{3})R30^{\circ}$ ,  $c(\sqrt{3} \times 7)rect$ ,  $c(4\times2)$ ,  $(4\times4)$  and  $(7\times7)$ , depending on the coverage of S. It was found that below 0.33 ML coverage, S occupies the fcc hollow site. Tensor LEED analyses [28] have been carried out for the  $(\sqrt{3} \times \sqrt{3})$ R30°-S and Rh(111)-c(4×2)-S surface structures formed by S chemisorbed at 1/3 and 1/2 ML coverages, respectively. For the lower coverage, S adsorbs on the fcc hollow site, and an S-Rh nearest neighbour bond distance was found to be 2.23 Å. The relaxations in the metal are negligible. In the  $c(4 \times 2)$  phase, the adsorption of S occurs equally on both types of hollow sites (fcc and hcp), and the average S-Rh bond length is 2.22 A. There are some relaxations in the metal. The surface structure of Rh(111)- $(\sqrt{3} \times \sqrt{3})$ R30°-S was also studied by NIXSW and SEXAFS [29]. The S atom was revealed to adsorb on the fcc hollow site, and the S-Rh bond length was found to be 2.25 Å.

CO adsorption on metal substrates has been the subject of numerous studies due to its simplicity and importance in catalysis. Adsorption of CO on Rh(111) also exhibits several ordered surface structures and its preferred adsorption site changes as the coverage is changed [30]. Core electron spectroscopy [31] has been used to investigate

Rh(111)-p(2×2)-CO and Rh(111)-( $\sqrt{3} \times \sqrt{3}$ )-R30°-CO, in which CO molecules were found to occupy the top sites in these structures. The geometrical structure of Rh(111)-( $\sqrt{3} \times \sqrt{3}$ )R30°-CO was well characterized by using tensor LEED combined with an automated optimization procedure analysis [30]. It revealed that CO occupies the top sites, excluding other high-symmetry sites. The C-O bond length was determined to be 1.20 Å and C-Rh is 1.87 Å.

Only a few S+CO coadsorption systems have been quantitatively determined. This is because firstly, the unit cells of such systems are usually quite large and therefore a full structure search is very time-consuming. Secondly, ordered phases in such systems are rare and relatively difficult to prepare experimentally.

Based upon the above structural information from experiments, CO chemisorption on Rh(111) in this study was modelled using a  $p(2 \times 2)$  unit cell with CO on the top site; S chemisorption was modelled using a  $p(2 \times 2)$  unit cell with S on the fcc hollow site; while the coadsorption system was modelled using a  $p(2 \times 2)$  unit cell with CO on the top site and S on the fcc hollow site. The geometry of Rh(111)-p(2 × 2)-(S+CO) is displayed in Fig. 1a. Although the experimental data are limited and there is no direct evidence for Rh(111)-

 $p(2\times2)$ -(S+CO) structure, some structural information still exists. Schwegmann et al.[32] obtained an ordered Rh(111)-p(2×2)-(O+CO) structure, in which O was found to sit on the fcc hollow position and CO occupies on the top site. Considering this structural information and that we are mainly interested in the interaction between CO and S, we believe that the choice of such a coadsorption system in Fig. 1a as a model is reasonable. Actually, there is another type of top site for CO in the  $p(2\times2)$  unit cell, shown in Fig. 1b. A recent study [33] on Pt(111)-p( $2 \times 2$ )-(O+CO) which is similar to Rh(111)-p(2×2)-(S+CO) showed that the top site for CO in Fig. 1a is more stable while the top site for CO in Fig. 1b is not stable at all (CO moves away from this top site once it is optimized).

We first performed the density functional theory calculations on Rh(111), Rh(111)-p(2×2)-CO, Rh(111)-p(2×2)-S and Rh(111)-p(2×2)-(S+CO). The possible tilting of CO was checked. It was found that the perpendicular configuration of CO on the surface is favoured on the unreconstructed Rh(111). The optimized structure parameters and the calculated chemisorption energies are summarized in Table 1. It can be seen that the S-Rh bond length of 2.25 Å in the Rh(111)-p(2×2)-S is equal to the S-Rh bond length which

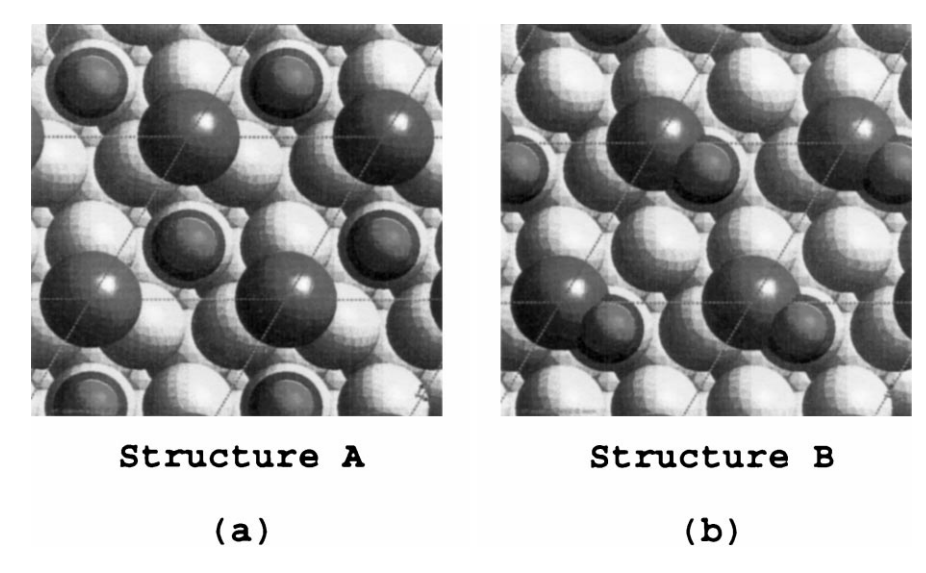


Fig. 1. Schematic illustration of geometrical structures for Rh(111)- $p(2 \times 2)$ -(S + CO). The  $p(2 \times 2)$  unit cell is indicated in dotted lines.

Table 1 Comparisons between structural parameters and chemisorption energies in Rh(111)-p(2×2)-(S+CO), Rh(111)-p(2×2)-CO and Rh(111)-p(2×2)-S: the corresponding results obtained from using eight k-points in the DFT calculations are given in parentheses, some structural parameters determined experimentally are also listed. The chemisorption energy of CO in Rh(111)-p(2×2)-(S+CO), namely the CO chemisorption energy in S-covered Rh(111), is calculated as  $\Delta E = E_{\text{total}}[Rh(111)-p(2\times2)-S]+E_$ 

C-O bond length (Å)	C-Rh bond length (Å)	S-Rh bond length (Å)	Chemisorption energy of CO (eV)	Chemisorption energy of S (eV)
1.16 (1.16)	1.86 (1.86)	2.25 (2.25)	1.60 (1.65)	5.05 (5.06)
1.10 (1.10)	1.00 (1.00)	2.25 (2.25)	1.00 (1.00)	5.25 (5.27)
		2.23 2.22		
1.20	1.87	2.25		
	length (Å)	length (Å) length (Å)  1.16 (1.16) 1.86 (1.86) 1.16 (1.16) 1.86 (1.86)	length (Å) length (Å) length (Å)  1.16 (1.16) 1.86 (1.86) 2.25 (2.25) 1.16 (1.16) 1.86 (1.86) 2.25 (2.25) 2.23 2.22 2.25	length (Å) length (Å) length (Å) of CO (eV)  1.16 (1.16) 1.86 (1.86) 2.25 (2.25) 1.60 (1.65) 1.80 (1.86) 2.25 (2.25) 2.23 2.22 2.25

was found for Rh(111) –  $(\sqrt{3} \times \sqrt{3})$ R30°-S [29], and the C-Rh bond length of 1.86 Å in Rh(111) $p(2\times2)$ -CO is almost identical with the value of 1.87 Å which was found in Rh(111) –  $(\sqrt{3} \times \sqrt{3})$ R30°-CO [30]. Compared to the free CO molecule, the C-O bond on Rh(111) is elongated, which is consistent with the generally accepted explanation that when CO adsorbs on metal surfaces, the C-O bond is weakened. Therefore, our calculated results are in good agreement with experiments. To check k-point convergence, we also performed calculations using eight k-points in the irreducible part of the surface Brillouin zone of a  $(2 \times 2)$  surface unit cell. The corresponding results are also listed in Table 1 for the sake of comparison. As it can be seen from Table 1, with increasing the number of k-points in the calculations, the changes of the local geometries such as S-Rh, C-Rh and C-O bond lengths are negligible. Moreover, the chemisorption energy differences between two k-points and eight k-points calculations are also very small. It is interesting that the increasing of the number of k-points has little effect on the S chemisorption energies [0.02 eV difference in Rh(111)-p(2 $\times$ 2)-S and 0.01 eV difference in Rh(111)-p(2 $\times$ 2)-(S+CO)] while the changes of CO chemisorption energies are relatively large [0.06 eV in Rh(111) $p(2 \times 2)$ -CO and 0.05 eV in Rh(111)- $p(2 \times 2)$ -(S+CO)].

A striking feature can be seen from Table 1:

The local geometrical structures of the coadsorption system such as the bond lengths of C-O, C-Rh and S-Rh are almost the same as those in Rh(111)-p(2×2)-CO and Rh(111)-p(2×2)-S, respectively. It was commonly held [1] that the main effect of an electronegative additive such as S on chemisorbed CO is to reduce the electron back donation from a metal surface to the CO  $2\pi$ antibonding orbital, since S could withdraw some electrons from the surface. Thus, one would expect to observe a stronger C-O bond, and a weaker C—Rh bond in the coadsorption system. However, our results show that the local geometry of CO is not affected by the presence of S, and vice versa. This indicates that the direct interaction between chemisorbed CO and S is very small in this system and that the bonding is local. In addition, the chemisorption energy of CO on S-covered Rh(111) decreases only by ca 0.2 eV in comparison to the pure CO on Rh(111), and the chemisorption energy of S on CO-covered Rh(111) is also reduced by  $\sim 0.2 \text{ eV}$  compared to the pure S on Rh(111). We can not rule out the effects of longrange electronic interaction. However, it is clear that a short-range interaction is dominant in this system.

We next investigated the structure of a larger unit cell (nine Rh atoms per layer with 1/9 S or CO surface coverage). Similarly to the above 1/4 ML coverage structure, we performed calculations on Rh(111), Rh(111)-p(3×3)-CO,

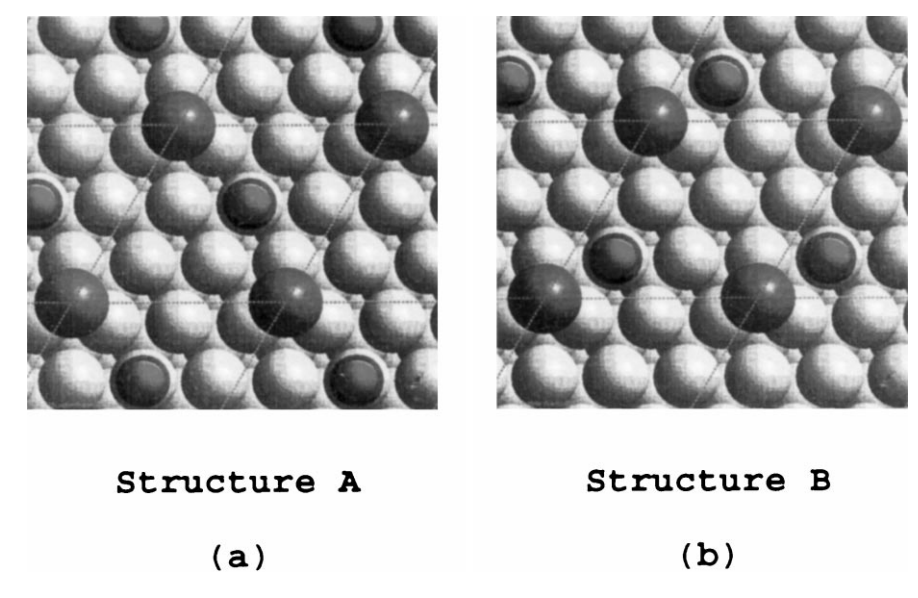


Fig. 2. Schematic illustration of geometrical structures for Rh(111)-p( $3 \times 3$ )-(S + CO). The p( $3 \times 3$ ) unit cell is indicated in dotted lines.

Rh(111)-p( $3 \times 3$ )-S and Rh(111)-p( $3 \times 3$ )-(S + CO) with S on the fcc hollow site and CO on a top site. In this case, two different top sites for CO adsorption were considered, one being shown in Fig. 2a, and the other in Fig. 2b. The optimized geometries and chemisorption energies are given in Table 2.

A comparison between Tables 1 and 2 shows that in the case of pure S on the Rh(111) surface, the sulfur chemisorption energy increases by 0.06 eV when S coverage is decreased from 1/4 to 1/9 ML. It indicates that the S—S interaction is repulsive. Likewise, the CO—CO interaction is also repulsive but to a lesser extent, since the chemisorp-

tion energy of CO increases only by  $0.02 \, \text{eV}$  with the decreasing of CO coverage from 1/4 to  $1/9 \, \text{ML}$  in the case of pure CO on the Rh(111) surface. Such repulsive interaction between CO molecules or S atoms tends to prevent the formation of CO islands or sulfur islands at low coverage. This is in agreement with the experimental conclusions in Ref. [12]. Concerning the interaction between CO and S in the  $p(3\times3)$  unit cell, the calculated results in Table 2 show that the CO chemisorption energy is reduced by ca  $0.05 \, \text{eV}$  upon coadsorption for CO on the top site which is more remote from the S atom (Fig. 2a), and it is reduced by ca  $0.1 \, \text{eV}$  for CO on the closer top site (Fig. 2b). We find

Table 2 Comparisons between the structural parameters and chemisorption energies in Rh(111)- $p(3 \times 3)$ -(S+CO), Rh(111)- $p(3 \times 3)$ -CO and Rh(111)- $p(3 \times 3)$ -S, where Rh(111)- $P(3 \times 3)$ -P(S+CO) (A) and Rh(111)- $P(3 \times 3)$ -P(S+CO) (B) refer to structures A and B in Fig. 2. Despite the fact that we did not check convergence with slab thickness and that the metal atoms were fixed in the calculations based on the computing cost consideration (very large unit cells were used here), the chemisorption energies and the local geometries should be reasonably accurate according to previous work [38,39]

	C-O bond length (Å)	C-Rh bond length (Å)	S-Rh bond length (Å)	Chemisorption energy of CO (eV)	Chemisorption energy of S (eV)
Rh(111)-p(3×3)-(S+CO) (A) Rh(111)-p(3×3)-(S+CO) (B) Rh(111)-p(3×3)-CO	1.16 1.16 1.16	1.86 1.86 1.86	2.25 2.25	1.83 1.78 1.88	5.29 5.24
$Rh(111)-p(3\times 3)-CO$ $Rh(111)-p(3\times 3)-S$	1.10	1.00	2.25	1.00	5.33

that structure A in Fig. 2 is a little more energetically favourable compared to structure B. This is because the CO is further away from the S atom in structure A, whereas the CO is quite close to one S atom in structure B. It is obvious that sulfur has a weak influence on the next nearest neighbour site, with the distance of 3.12 Å. It is also clear that the interaction between CO and S in a  $p(2 \times 2)$ unit cell is a little larger than that in a  $p(3 \times 3)$ unit cell. However, it should be addressed that the decrease of adsorption energy of CO and S upon coadsorption is very small. As one can see from Tables 1 and 2, the C-Rh and C-O bond length is not affected by the presence of sulfur, and the S-Rh bond length is also not affected by the presence of CO. Thus, we can conclude that the bonding is very local in these systems.

The LDOS shows an energy-resolved charge density distribution for a system which is usually obtained by projecting individual quantum states into a local region such as an atom. It has been widely used for electronic structure analysis. In order to further understand the results discussed above, we calculated LDOS around CO. In our calculations, the amount of electron density in each quantum state of a system, which lies within a cylinder around CO with a radius of 1.0 Å, was determined, and then the amount of electron density versus the energy of the quantum state was plotted. The LDOS around CO for Rh(111) $p(3 \times 3)$ -CO and Rh(111)- $p(3 \times 3)$ -(S+CO) are shown in Fig. 3, in which structure A in Fig. 2a and structure B in Fig. 2b are donated by S/CO/Rh (A) and S/CO/Rh (B), respectively. By examining the quantum states in CO/Rh(111), we found that the first peak in Fig. 3a has a strong CO  $3\sigma$  orbital character and the second peak mainly contains a CO  $4\sigma$  character with a weak metal d-character. The third peak centered at 7 eV below  $E_f$  was found to consist of two types of states:

- 1. mixing states with strong CO  $1\pi$  and weak metal d-character;
- 2. mixing states with strong CO  $5\sigma$  and quite strong metal d-character.

The quantum states in the peak above  $E_{\rm f}$  mainly contain a strong  $2\pi$  character of CO and metal d-character. Experimentally, ultraviolet photoelectron spectra of adsorbed CO on a Rh(111)

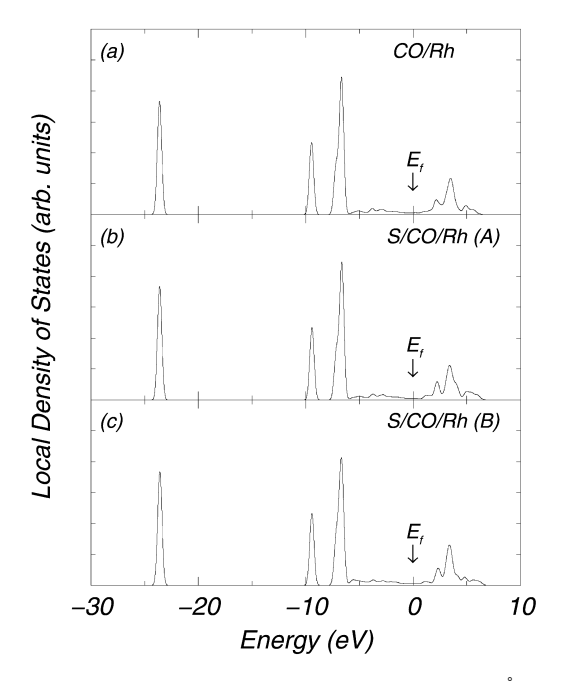


Fig. 3. LDOS cutting around CO with a radius of 1.0 Å from Rh(111)-p( $3 \times 3$ )-CO, Rh(111)-p( $3 \times 3$ )-(S+CO) (A) and Rh(111)-p( $3 \times 3$ )-(S+CO) (B).

surface [34] were measured, and two peaks centered at binding energies, 7.9 and 10.8 eV, were observed. These two peaks were assigned to the molecular orbitals,  $1\pi/5\sigma$  and  $4\sigma$ , respectively. Our calculation results are consistent with these observations. Comparing the LDOS for Rh(111) $p(3 \times 3)$ -CO with that for the coadsorption systems, it is evident that the local densities of states around CO for these three systems displayed in Fig. 3 are very similar. The number of peaks, the peak shape and the peak positions in these systems are almost identical. This result further supports the suggestion that the interaction between chemisorbed CO and S is very small and the bonding is very local in these systems. However, our results are not entirely consistent with previous work [18]. The LDOS projected on a C atom from an allelectron local-density-functional theory study for Ni(100)-c(2×2)-CO and Ni(100)-c(2×2)-(S+CO) [18] showed that the  $1\pi/5\sigma$  band is markedly broadened from 1 eV for CO/Ni to 2.5 eV for (S+CO)/Ni, and the  $4\sigma$  peak shifts slightly downwards in (S+CO)/Ni compared to CO/Ni. A possible explanation for the discrepancy might be that the unit cell they used is smaller than ours. In such a small unit cell as  $c(2 \times 2)$ , the CO molecule and the S atom can bond directly with the same metal atom, and a direct strong repulsion due to bonding competition will form, which surely can significantly affect the density of states around CO. In order to further confirm our results, we also calculate the LDOS around S for Rh(111)-p(3×3)-S and Rh(111)-p(3×3)-(S+CO) (both structures A and B in Fig. 2). A cylinder around S with a radius of 1.1 Å was used in the calculations. In Fig. 4 the LDOS around S for Rh(111)-p(3×3)-S and Rh(111)-p(3×3)-(S+CO) are compared. The similarity between these three curves is also obvious. Therefore, the weak interaction between CO and S does not significantly affect the LDOS around either CO or S.

The weak interaction between CO and S can be further seen in the total valence charge density distributions. Fig. 5a and b show two-dimensional contour plots of the total valence charge densities

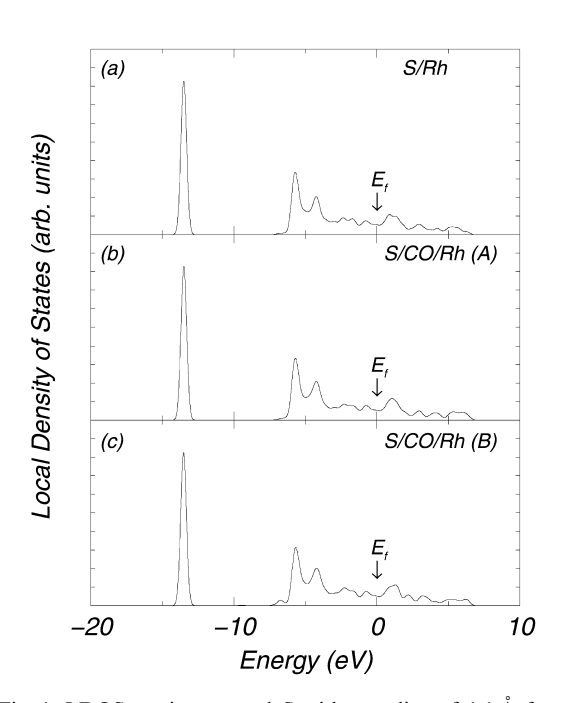


Fig. 4. LDOS cutting around S with a radius of 1.1 Å from Rh(111)-p( $3\times3$ )-CO, Rh(111)-p( $3\times3$ )-(S+CO) (A) and Rh(111)-p( $3\times3$ )-(S+CO) (B).

in a cut through the CO and S atoms from the structures A and B illustrated in Fig. 2, respectively. The same cuts from Rh(111)-p( $3 \times 3$ )-CO and Rh(111)-p( $3 \times 3$ )-S are displayed in Fig. 5c and d, respectively. It shows clearly that the chemisorbed S atom or the CO molecule does not significantly affect the charge distribution of the next nearest neighbours. These features are quantitatively confirmed by the results in Table 3, in which the total valence electrons in a certain spheres around the C, O and S atoms are listed. A radius of 1.1 Å, which is about the distance from a S atom center to the charge density minimum along the metal-S bond axis, is chosen for the S atom in order to avoid cutting into metal atoms. The radius of 0.4 Å and 0.7 Å for C and O atoms are chosen for the same reason. It can be seen that the charges around S, C and O in structure A are the same as those in Rh(111) $p(3 \times 3)$ -S and Rh(111)- $p(3 \times 3)$ -CO, respectively. For structure B, there is also no significant change in comparison with pure CO on metal or pure S on metal. It is obvious that the presence of S does not significantly influence the charge density distribution around CO, and vice versa.

## 4. Discussion

Goodman and co-workers carried out kinetic studies [3–5] and showed clearly that a 0.1 ML coverage of S could reduce dramatically the CO methanation rate. There are two possible explanations for this long range S poisoning effect:

- 1. extended electronic effect, which means that the electronic structures of neighbour metal atoms (up to 3.12 Å away from S) are changed substantially due to the S chemisorption; and
- 2. ensemble effect, namely that a certain number of active surface atoms are required to facilitate the reaction sequence.

The need for such ensembles in catalysis was previously proposed [35]. A kinetic study on the CO methanation reaction on Ni/SiO<sub>2</sub> catalysis [36] also showed the importance of the ensemble effect. However, if an ensemble of metal atoms is required for the CO methanation, one would expect that altering the electronegative character of poisoning

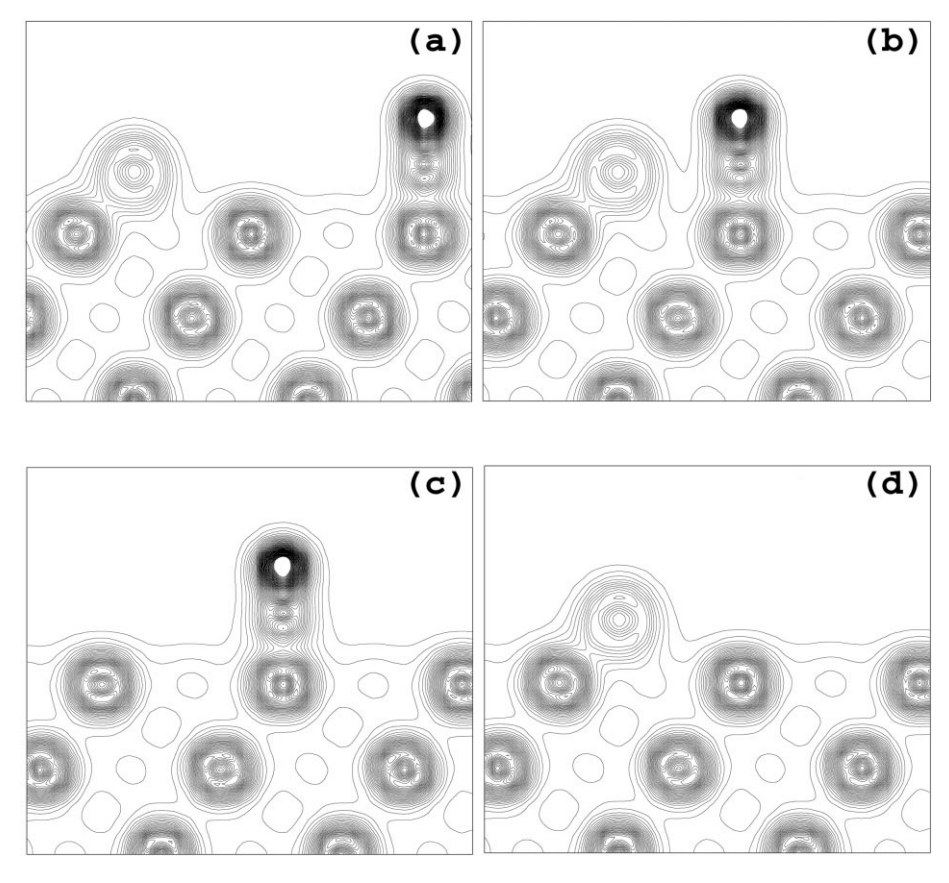


Fig. 5. (a) and (b) show two-dimensional contour plots of the total valence charge densities in a cut through the CO and S atoms from structures A and B illustrated in Fig. 2, respectively. The same cuts from  $Rh(111)-p(3\times3)-CO$  and  $Rh(111)-p(3\times3)-S$  are displayed in (c) and (d), respectively.

Table 3 Total valence electrons in volumes cutting around S, C and O atoms in Rh(111)-p( $3\times3$ )-(S+CO) (A), Rh(111)-p( $3\times3$ )-(S+CO) (B), Rh(111)-p( $3\times3$ )-CO and Rh(111)-p( $3\times3$ )-S. The radius of 1.1 Å is chosen for the S atom because it is approximately the distance between a S atom center and the minimum valence electron density along the Rh—S bond axis, the radii of 0.7 Å for O and 0.4 Å for C atom were used for the same reason

	S	C	О
$Rh(111)-p(3\times3)-(S+CO)(A)$	4.14	0.41	4.21
$Rh(111)-p(3\times3)-(S+CO)$ (B)	4.10	0.41	4.18
Rh(111)-p(3×3)-CO	4.1.4	0.41	4.21
$Rh(111)-p(3\times3)-S$	4.14		

species should not considerably change the poisoning effect. Kiskinova and Goodman [4] found that this is not true for the CO methanation on the Ni(100) surface. They showed that substituting phosphorus for sulfur resulted in a marked change in the magnitude of the poisoning effect, namely, the poisoning effect of phosphorus is considerably less dramatic than that of sulfur at low coverage. Based on these results, they suggested, therefore, that the poisoning effect is related to the electronegativity of adsorbates and the S long range poisoning effect is due to the extended electronic effect.

However, the explanation of extended electronic effect for the S long range poisoning is not consistent with our results. A recent study shows [33]

that a chemisorbed O atom can 'poison' three nearest neighbour metal atoms when the O atom sits on a hollow site of Pt(111) while it does not have any significant influence on the next nearest neighbour sites. As we reported in Section 3, a chemisorbed S atom almost does not affect the local geometry of chemisorbed CO on the next nearest neighbour site at all [no change of C-O and C-metal bond lengths in Rh(111)-p( $3 \times 3$ )-(S+CO) compared to Rh(111)-p(3×3)-CO]. The chemisorption energy of CO on the next nearest neighbour site is only reduced by 0.1 eV (<2%) due to the presence of sulfur. Our results suggest that chemisorbed S atoms do not considerably influence the reactivity of any site for CO chemisorption once they are beyond the next nearest neighbours.

There are in fact several elemental steps in the CO methanation: CO chemisorption; CO dissociation; H2 dissociation; and hydrogenation of surface carbon or intermediates. At the moment, we only have evidence that the chemisorbed S atoms do not significantly 'poison' CO chemisorption beyond the next nearest neighbour sites. In other words, the extended electronic effect due to S chemisorption is not important for the CO chemisorption. Whether the extended electronic effect of S strongly influences the other elemental steps is an open question. However, we would guess that it is not important either. Then how can one explain the S long range poisoning effect on the CO methanation? We tend to believe that it is due to an ensemble effect. It appears that the  $p(3 \times 3)$ unit cell (the S coverage is 1/9, being close to the low limit of the experiment) is quite small for the elemental steps in the CO methanation mentioned above. Suppose that the methanation occurs in the following sequence, for example:

- 1. CO dissociation;
- 2. H2 dissociation; and
- 3. hydrogenation, and further suppose that the C and O atoms occupy the hollow sites after the CO dissociation process, then it is expected that the hydrogen dissociation will be hindered in terms of bonding competition [37].

If any of the elemental steps were dramatically hindered, the overall reaction will be poisoned. If this is true, one may expect many elements such as Cl and P should poison the methanation in the same manner. In other words, P chemisorption should, for example, reduce dramatically the methanation reaction rate when P coverage is as low as 0.1 ML. This is, in fact, inconsistent with the experimental observation of Kiskinova and Goodman [4]. How can we explain the quite different poisoning effects of P and S? One possible explanation is that adsorption of P may form islands or a sort of islands so that a large surface area is not affected while S adsorption may have quite a uniform distribution even at low coverage. It should be stressed that the viewpoint above is obviously oversimplistic and more detailed work is required. In any event, we believe that the extended electronic effect for the explanation of the S long range poisoning effect is likely to be incorrect.

## 5. Conclusion

The CO-S interaction on Rh(111) surface has been investigated theoretically. Geometrical structures of Rh(111)-p(2 $\times$ 2)-CO, Rh(111) $p(2 \times 2)$ -S, Rh(111)- $p(2 \times 2)$ -(S+CO), Rh(111) $p(3\times3)$ -CO, Rh(111)- $p(3\times3)$ -S and Rh(111) $p(3\times3)$ -(S+CO) are optimized and chemisorption energies are determined using DFT. The results show that the C-O, Rh-C and Rh-S bonds in the coadsorption system are almost the same as those in pure CO on Rh(111) or pure S on Rh(111), respectively. The chemisorption energies of CO are not considerably affected by the presence of sulfur, and vice versa. The total valence charge density distributions around C-O and S in the coadsorption systems are also very similar to those in pure CO or pure S on Rh(111), respectively. There are clear similarities in the LDOS cutting around CO between CO/Rh(111) and S/CO/Rh(111). Similarities of the LDOS cutaround S between S/Rh(111) and S/CO/Rh(111) also exist. All these provide evidence that the bonding is local and the interaction between adsorbates is mainly short range in nature. Based this short-range mechanism, it is concluded that an ensemble effect that requires a certain number of active surface atoms to facilitate the reaction sequence, rather than the electronic effect, may be responsible for the reduction of the CO methanation rate.

## Acknowledgement

This work has been supported by the EPSRC.

## References

- [1] M. Kiskinova, Surf. Sci. Rep. 8 (1988) 359.
- [2] D.W. Goodman, J. Phys. Chem. 100 (1996) 13090.
- [3] D.W. Goodman, M. Kiskinova, Surf. Sci. 105 (1981) L265.
- [4] M. Kiskinova, D.W. Goodman, Surf. Sci. 108 (1981) 64.
- [5] D.W. Goodman, Appl. Surf. Sci. 19 (1984) 1.
- [6] W. Erley, H. Wagner, J. Catalysis 53 (1978) 287.
- [7] D.W. Goodman, Heterogeneous Catalysts (Proceedings of IUCCP Conference), Texas A&M University, Texas, 1984.
- [8] C.H.F. Peden, D.W. Goodman, in: M.L. Devinny, J.L. Gland (Eds.), Proceedings of Symposium on the Surface Science of Catalysts, Philadelphia American Chemical Society, Washington, DC, 1984..
- [9] R.J. Madix, M. Thornburg, S.B. Lee, Surf. Sci. 133 (1983) L447.
- [10] J.L. Gland, R.J. Madix, R.W. McCabe, C. DiMaggio, Surf. Sci. 143 (1984) 46.
- [11] M. Trenary, K.J. Uram, J.T. Yates, Surf. Sci. 157 (1985) 512.
- [12] P. Sprunger, F. Besenbacher, I. Stensgaard, E. Lagsgaard, Surf. Sci. 320 (1994) 271.
- [13] P.J. Feibelman, D.R. Hamann, Phys. Rev. Lett. 52 (1984) 61.
- [14] P.J. Feibelman, D.R. Hamann, Surf. Sci. 149 (1985) 48.
- [15] J.M. Maclaren, J.B. Pendry, Surf. Sci. 178 (1986) 856.

- [16] N.D. Lang, S. Holloway, J.K. Nørskov, Surf. Sci. 150 (1985) 24.
- [17] J.K. Nørskov, S. Holloway, N.D. Lang, Surf. Sci. 137 (1984) 65.
- [18] E. Wimmer, C.L. Fu, A.J. Freeman, Phys. Rev. Lett. 55 (1985) 2618.
- [19] S. Wilke, M. Scheffler, Surf. Sci. 329 (1995) L605.
- [20] S. Wilke, M. Scheffler, Phys. Rev. Lett. 76 (1996) 3380.
- [21] D. Vanderbilt, Phys. Rev. B 41 (1990) 7892.
- [22] P. Hu, D.A. King, S. Crampin, M.H. Lee, M.C. Payne, Chem. Phys. Lett. 230 (1994) 501.
- [23] P. Hu, D.A. King, M.H. Lee, M.C. Payne, Chem. Phys. Lett. 246 (1995) 73.
- [24] P. Hu, D.A. King, S. Crampin, M.H. Lee, M.C. Payne, J. Chem. Phys. 107 (1997) 8103.
- [25] D.M. Ceperley, B.J. Alder, Phys. Rev. Lett. 45 (1980) 566.
- [26] J.P. Perdew, in: P. Ziesche, H. Eschrig (Eds.), Electronic Structure of Solids, Akademie Verlag, Berlin, 1991.
- [27] H.A. Yoon, M. Salmeron, G.A. Somorjai, Surf. Sci. 395 (1998) 268.
- [28] K.C. Wong, W. Liu, M. Saidy, K.A.R. Mitchell, Surf. Sci. 345 (1996) 101.
- [29] A. Santoni, B.C.C. Cowie, G. Scarel, V.R. Dhanak, Surf. Sci. 388 (1997) 254.
- [30] M. Gierer, A. Barbieri, M.A. Van Hove, G.A. Somorjai, Surf. Sci. 391 (1997) 176.
- [31] A. Beutler, E. Lundgren, C. Nyholm, J.N. Andersen, B. Setlik, D. Heskett, Surf. Sci. 371 (1997) 381.
- [32] S. Schwegmann, H. Over, V. De Renzi, G. Ertl, Surf. Sci. 375 (1997) 91.
- [33] K. Bleakley, P. Hu, J. Am. Chem. Soc. (1999) submitted.
- [34] J. Kiss, G. Klivenyi, K. Revesz, F. Solymosi, Surf. Sci. 223 (1989) 551.
- [35] J. Sinfelt, Bimetallic Catalysts, Wiley/EXXON, Chichester, 1983.
- [36] J.A. Dalmon, G.A. Martin, J. Catalysis 84 (1983) 45.
- [37] A. Alavi, P. Hu, T. Deutsch, P.L. Silvestrelli, J. Hutter, Phys. Rev. Lett. 80 (1998) 3650.
- [38] G. te Velde, E.J. Baerends, Chem. Phys. 177 (1993) 399.
- [39] A. Michaelides, P. Hu, A. Alavi, J. Chem. Phys. in press.